

UNIVERSITY OF SOUTHERN CALIFORNIA

DEPARTMENT OF CIVIL ENGINEERING

TIME OF MAXIMUM RESPONSE OF SINGLE-DEGREE-OF-FREEDOM  
OSCILLATOR TO EARTHQUAKE EXCITATION

by

Vincent W.-S. Lee and Mihailo D. Trifunac

Report No. CE 79-14

A Report on the Research Conducted Under a Contract  
from the U.S. Nuclear Regulatory Commission

Los Angeles, California

October, 1979



TIME OF MAXIMUM RESPONSE OF SINGLE DEGREE-OF-FREEDOM  
OSCILLATOR TO EARTHQUAKE EXCITATION

by

V.W. Lee and M.D. Trifunac

ABSTRACT

The dependence of the relative time of maximum response of single degree-of-freedom system, subjected to recorded strong earthquake ground motion, on magnitude, epicentral distance and the Modified Mercalli Intensity at the site has been studied. Two empirical regression models are presented that enable estimation of the time of maximum response in terms of (1) earthquake magnitude and epicentral distance, or (2) Modified Mercalli Intensity at the site. The distribution function of the observed times of maximum response is also derived. Both models also consider whether motion is horizontal or vertical, and the effects of the geologic conditions surrounding the site. The results are useful for the response spectrum approach in earthquake resistant design, as they provide guidelines for superposition of different loads in time.



## INTRODUCTION

In response spectrum calculations, the times at which maxima occur are usually not considered. In a typical response spectrum approach, when computing an estimate of the maximum response of a multi-degree-of-freedom system by adding individual mode responses it is assumed that it is possible, though not very likely, that all mode responses can experience maximum response at the same time. Depending on the type of the analysis (a) the square root of the sum of the squared maximum responses of individual modes, or (b) the absolute sum of maximum mode responses, is used to represent the maximum response of the whole system.

For certain applications, however, it is advantageous to consider the times when maxima of mode responses occur in a multi-degree-of-freedom systems and to use this information to better describe the response of the complete system. To illustrate possible uses of such approach, we present the following two examples.

First, we consider the estimation of the maximum response in a system which has low frequency of the fundamental mode and relatively high frequencies of second and higher modes. When the duration of high-frequency strong shaking is short relative to the period of the first mode, the maxima of the higher mode responses for such a system may all be achieved well before the fundamental mode goes through its maximum response. Under such circumstances, both methods (a) and (b) above for computing the overall maximum response then lead to overestimates of the maximum response of the whole system.

In the second example the superposition of earthquake induced loads to the loads which may result from the increase in containment pressure following a hypothetical accident in nuclear power plants is considered. These two loads are usually superimposed in calculations of maximum member stresses involving conditions assumed for the safe shutdown earthquake (SSE). If it is realized, however, that maximum accident containment pressure caused by earthquake shaking can take some time to develop, it is easy to see that under favorable conditions, by the time these pressure stresses reach their largest values, the dynamic stresses induced by earthquake shaking may be already diminished. Hence, assuming that these two loading conditions contribute concurrently to the maximum response may lead to higher actual safety factors for building structures but may not be appropriate for estimating response of all equipment mounted to these structures.

The above examples suggest that detailed knowledge of when the maximum mode responses occur is helpful to understand in more detail the nature of response of the multi-degree-of-freedom systems subjected to earthquake excitation. To this end, in this paper we present two empirical models for estimation of this time in terms of (a) earthquake magnitude and epicentral distance and (b) Modified Mercalli Intensity at the site. We restrict this analysis to characterization of the time of maximum response of the viscously damped single-degree-of-freedom system as excited by recorded strong ground motion. As a result, the models presented here are limited in their applicability to those intervals of the independent scaling variables for which the data is now available.

Attempts were made [1] to describe the time of maximum response of a single-degree-of-freedom system in terms of the probability of the first passage. However, this difficult problem has not yet been solved and only some approximate theoretical models are currently available [1]. The analysis of this problem from an empirical viewpoint in this paper, and based on actual observations, may thus prove useful in further theoretical studies.

## DATA BASE AND REGRESSION

The data base for this analysis consists of 186 records of strong ground motion in the western United States, each consisting of two horizontal acceleration traces and one vertical trace. These accelerograms were recorded during the period between 1933 and 1971 and constitute so far the largest uniformly processed group of strong motion records any place in the world. Though incomplete in many respects, this data set has already proved to be the invaluable basis for analyses focusing on the detailed characterization of strong ground shaking [4,5,6,7,8,9].

In routine computation of relative displacement (SD) response spectra [3], the ordinates of Response Envelope Spectra (RES) [2] consisting of amplitude and time coordinates of all maxima of the responses of 91 single-degree-of-freedom, viscously damped oscillators have been stored onto a magnetic tape. By plotting RES amplitudes versus time and frequency, it is possible to derive information on how relative motions of different oscillators respond in time to recorded strong motion acceleration. In Figure 1, an example of such RES for  $\omega * SD$  (where  $\omega = 2\pi/T$  and  $T$  is the undamped period of single-degree-of-freedom system) is shown for acceleration recorded at 646 S. Olive Avenue in Los Angeles, recorded during the San Fernando, California, earthquake of 1971. The RES contours show the changes of response amplitudes in time and frequency.

Heavy irregular line in Figure 1 starting just after 10 seconds at the high frequency end of RES plot and fluctuating first back to about

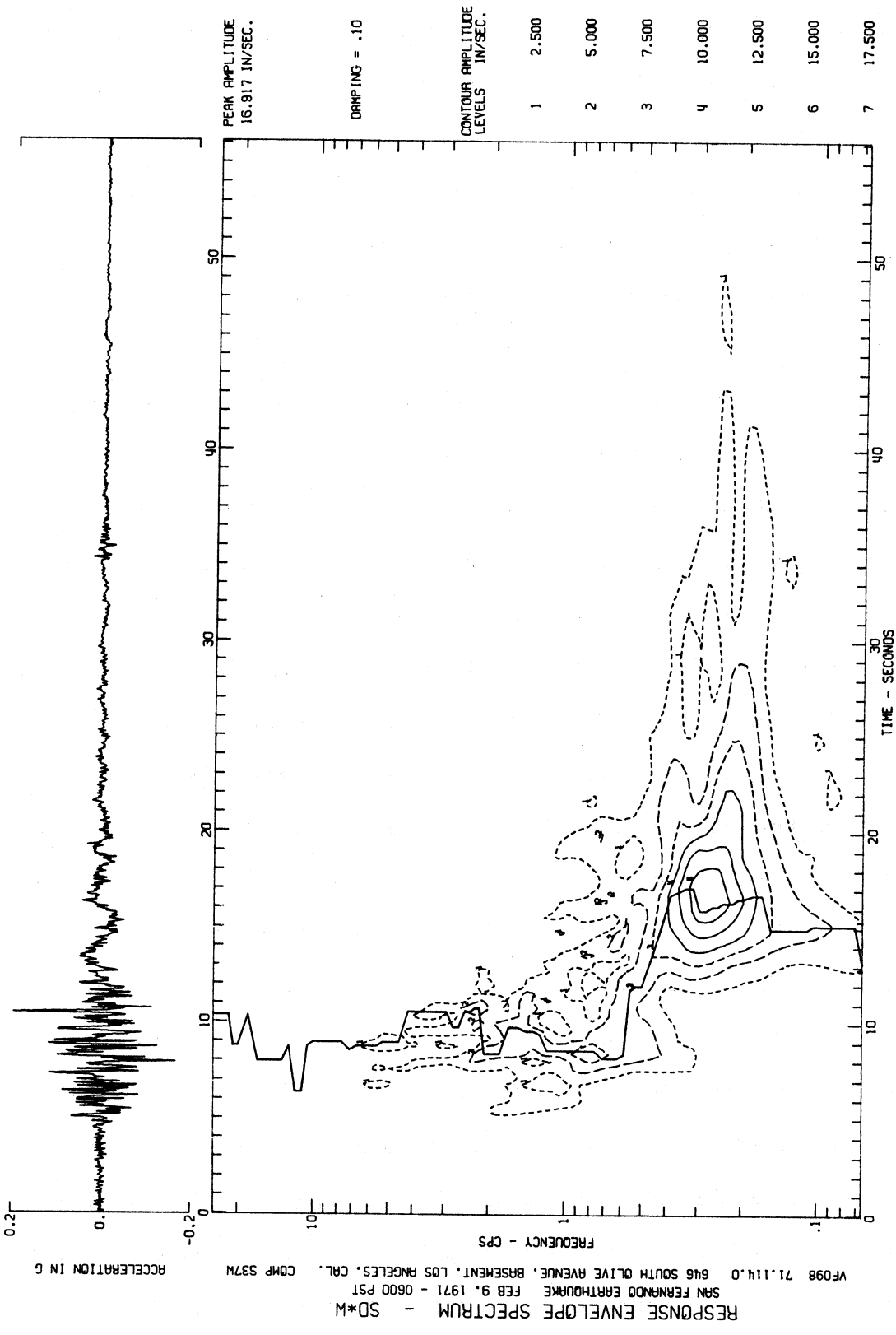


FIGURE 1

6 sec at the frequency of about 10 cps and then migrating towards the time interval between 15 and 20 seconds for frequencies less than 1 cps indicates the times of maximum responses for each of oscillators at 91 different periods (between 0.04 sec and 15 sec) and for the fraction of critical damping  $\zeta = 0.10$ . The amplitudes of RES along this line plotted versus frequency,  $f$ , or period  $T = 1/f$ , would result in the Pseudo Relative Velocity Spectrum ( $PSV = \omega * SD$ ) which is frequently used in earthquake resistant design based on the response spectrum superposition approach [9].

For all 186 records (372 horizontal and 186 vertical accelerograms) we calculated Response Envelope Spectra at 91 periods ranging from 0.04 sec to 15 seconds and for damping  $\zeta = 0.00, 0.02, 0.05, 0.10$  and  $0.20$ . This resulted in 2790 RES spectra of which the spectrum in Figure 1 is an example. From these RES spectra, the times of maximum response versus 91 frequencies were extracted for subsequent analysis.

The distribution of data among five magnitude intervals is as follows: 3.0 to 3.9, 1 record; 4.0 to 4.9, 5 records; 5.0 to 5.9, 40 records; 6.0 to 6.9, 120 records; 7.0 to 7.9, 7 records and unknown magnitudes, 4 records. The distribution of data among seven intensity levels is as follows: MMI = II, 1 record; MMI = IV, 3 records; MMI = V, 34 records; MMI = VI, 66 records; MMI = VII, 75 records; MMI = VIII, 6 records; and MMI = X, 1 record. The majority of recordings (117) were registered on stations located in alluvium and sedimentary deposits (classified as  $s=0$ ; see reference 4 for a detailed description of this classification and for examples of assigning  $s=0, 1$  or  $2$  to selected sites), 52 records

came from sites located on intermediate type rocks ( $s=1$ ), and only 13 records from stations on basement rock ( $s=2$ ).

#### Scaling in Terms of $M$ , $\Delta$ , $s$ , $v$ and $p$

For damping values  $\zeta = 0.02, 0.05, 0.10$  and  $0.20$ , we select

$$TMAX(T),_p = a(T)p + b(T)s + c(T)M + d(T)\Delta + e(T)v \quad (1)$$

where  $TMAX(T),_p$  is the relative time of maximum response of the single-degree-of-freedom, viscously damped, oscillator (with natural period  $T$ ), that will not be exceeded in  $100p$  percent cases.  $p$  is not probability, but through term  $a(T)p$  represents a linear approximation to the actual distribution of  $TMAX(T)$  about the regression model (1) when  $0.05 \leq p \leq .95$ .  $s$  represents the site conditions.  $M$  is the magnitude which for most earthquakes with  $M \lesssim 6.5$  in the data set of 57 earthquakes considered here [4] represents the local Richter magnitude  $M_L$ .  $\Delta$  is epicentral distance in kilometers and  $v$  represents component direction to which  $TMAX(T),_p$  applies ( $v=0$  for horizontal and  $v=1$  for vertical motion). Functions  $a(T)$  through  $e(T)$  are the scaling functions of  $T$  and are determined from the regression analysis.

The functional form of equation (1) has been motivated by the studies of duration of strong shaking [6,7] which have argued that duration is a linear function of  $R$ . The term  $c(T)M$  represents a linear approximation to what should be an exponential dependence on  $M$  as suggested by simple models of earthquake sources involving propagating dislocations.

Many recorded strong motion accelerograms contain what could be identified as clear S-wave arrivals. This is particularly the case for more recent recordings which come from accelerographs with vertical

triggering devices. These are often triggered by the P-wave or some of its latter reflections but well before the S-wave arrival. In some cases, primarily for older recordings of small and more distant earthquakes, the S-wave arrivals may be difficult to identify because of their proximity to the triggering time or because of the late triggering by means of penduli sensitive predominantly to horizontal motions.

To provide a uniform physical basis for  $TMAX(T)$  in (1) it is necessary to select origin for the time coordinate on each recorded accelerogram and to measure  $TMAX(T)$  relative to this origin. However, unique choice of such origin is not possible since selection of S-wave arrival time, for example, is subject to some judgement and the experience of an analyst. Furthermore, for mode superposition approach in earthquake resistant design, only the relative times of maximum responses of each mode are required.

Detailed study of many RES spectra shows that the high frequency oscillators will reach maximum response immediately or soon after the S-wave arrival time. In Figure 1, for example, it is seen that the responses of several oscillators with natural frequency near 10 cps reach maxima of  $\omega * SD$  within 1 or 2 seconds after the S-wave arrival, in this example, at about 4.5 seconds after triggering. Therefore, one simple and reproducible way of measuring the relative time of maximum response is to compute it with respect to the earliest time of all maximum responses considered in the frequency band between 0.07 cps and 25 cps. In Figure 1 the origin for measuring the time of maximum response would thus be at about 6.5 seconds. This definition of  $TMAX(T)$  has been adopted for this analysis and 91 time coordinates in 558 RES have been shifted by  $\min[TMAX(T)] \forall 0.04 < T < 15$ .

For high natural frequencies of single-degree-of-freedom system and for band limited excitations, the maximum relative response tends to  $-a_{\max}(t)/\omega_n^2$ .  $a_{\max}(t)$  is the peak absolute acceleration and  $\omega_n = 2\pi/T_n$ . Since all uniformly processed strong motion data have been band-pass filtered between 0.07 cps and 25 cps, the time of maximum response in RES spectra for 25 cps should correspond to the time of maximum input acceleration (Figure 1). Thus, in this analysis, TMAX(0.04) then gives the relative time of the peak absolute acceleration.

To compute the scaling functions  $a(T)$  through  $e(T)$  all data was partitioned into groups corresponding to magnitude ranges 4.0 to 4.9, 5.0 to 5.9, 6.0 to 6.9 and 7.0 to 7.9. These groups were further divided into three sub-groups corresponding to site classification  $s=0, 1$  and  $2$ . Each of these sub-groups was finally subdivided into two parts corresponding to  $v=0$  and  $v=1$ . Within each of these parts,  $n$  data points on TMAX(T) were rearranged to create a monotonically decreasing sequence. With  $m$ -integer part of  $(pn)$  and  $0.05 \leq p \leq 0.95$  the  $m^{\text{th}}$  data point then represents an estimate of an upper bound on TMAX(T) for which  $100p$  percent of the corresponding data set is less than that value. In regression calculations, at most 19 values of  $p=0.05, 0.10, \dots, 0.90$  and  $0.95$  were used to eliminate strong dependence of the final regression model on those earthquakes which contributed most to the present data set. For example, the San Fernando earthquake of 1971 contributed 98 to the total of 186 records. The above method of data selection eliminated about 70 percent of the San Fernando records before regression analysis at each T.

Figure 2 and Table I present smoothed coefficient functions  $a(T)$  through  $e(T)$ . Function  $a(T)$  shows that the 80 percent confidence interval for  $T_{MAX}(T)$  is about 5 to 6 seconds wide for  $T < 0.5$  sec. For two second period, this interval is extended well over 20 seconds. Function  $b(T)$  shows that maxima occur 1 to 2 seconds earlier for sites located on basement rock ( $s=2$ ) than on alluvium sites ( $s=0$ ) and for  $f \geq 5$  cps. For long periods near 2 seconds, this difference increases to as much as 10 seconds. This means that the duration of strong motion acceleration should be greater for sites located on alluvium relative to sites on hard rock. This is in agreement with the work of Trifunac and Westermo (1976).

Function  $c(T)$  shows a decrease in  $T_{MAX}(T)$  with magnitude,  $M$ , by less than 1 second over the magnitude range from  $M=4$  to  $M=7$ . This apparently minor effect of magnitude on  $T_{MAX}(T)$  could be interpreted to mean that the initial bursts of strong motion pulses created by larger magnitude earthquakes are more energetic and more abrupt so that the maximum response is achieved earlier relative to intermediate and small magnitude events.

Function  $d(T)$  indicates that the maximum response is delayed by 1 to 2 seconds for every additional 10 km of epicentral distance,  $\Delta$ , and for periods shorter than about 1 second, and by 3 to 5 seconds for periods longer than 2 seconds. This is as one could expect from the dispersion of wave motion with distance.

Function  $e(T)$  shows that the maximum vertical response occurs 1 to 5 seconds later than the maximum of horizontal response. In terms of the natural period and of the single-degree-of-freedom system, this

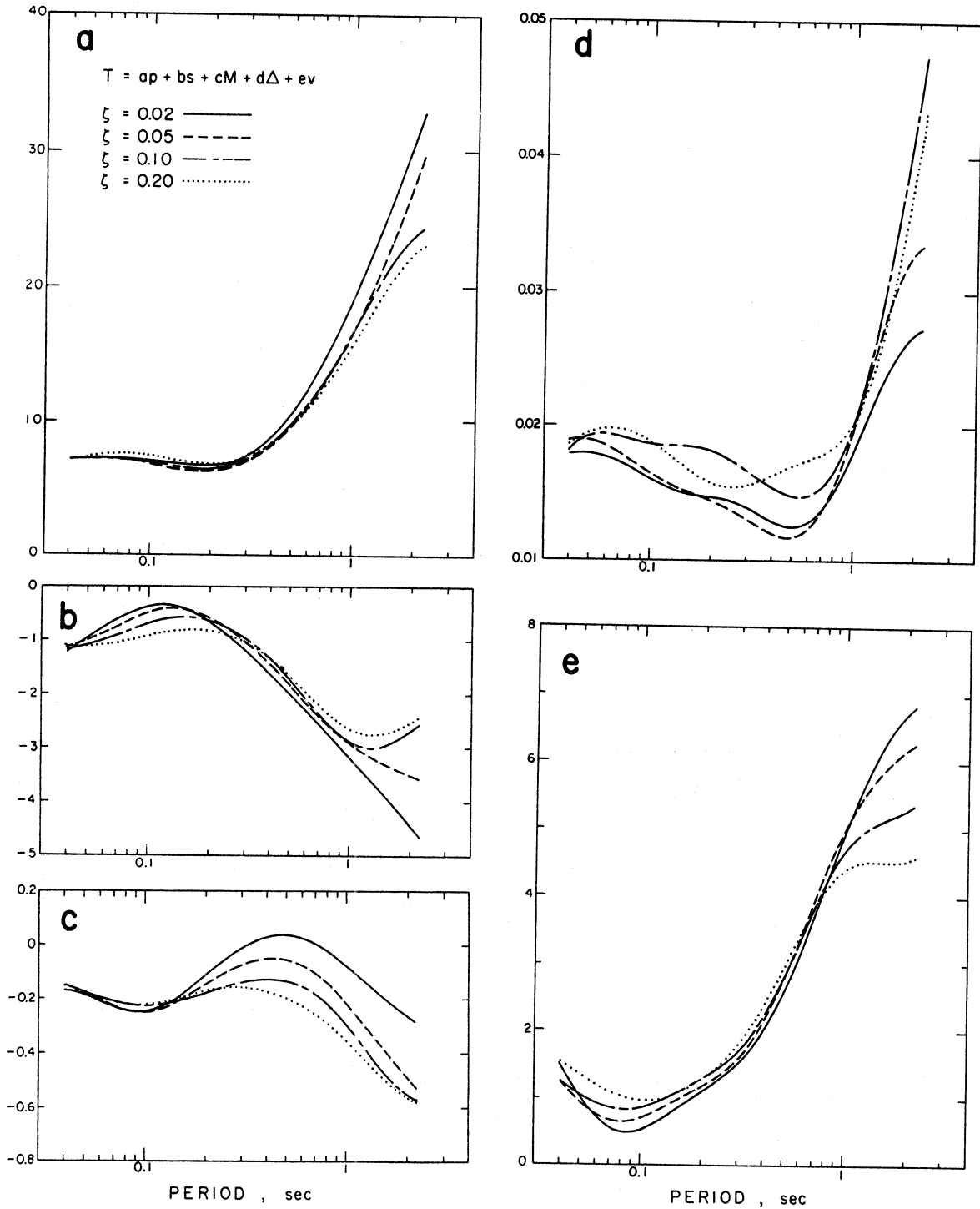


FIGURE 2

Functions  $a(T)$ ,  $b(T)$ , ... and  $e(T)$  in  
 $T_{MAX}(T) = a(T)p + b(T)s + c(T)M + d(T)\Delta + e(T)v$

TABLE I

Coefficient Functions  $a(T)$  through  $e(T)$  in  $TMAX(T)$ ,  $p = a(T)p + b(T)s + c(T)M + d(T)\Delta + e(T)v$   
for Four Fractions of Critical Damping  $\zeta$

| T<br>(sec) | a(T) |      |      |      | b(T)  |       |       |       | c(T)  |       |       |       | d(T) |      |      |      | e(T) |      |      |      |
|------------|------|------|------|------|-------|-------|-------|-------|-------|-------|-------|-------|------|------|------|------|------|------|------|------|
|            | 0.02 | 0.05 | 0.10 | 0.20 | 0.02  | 0.05  | 0.10  | 0.20  | 0.02  | 0.05  | 0.10  | 0.20  | 0.02 | 0.05 | 0.10 | 0.20 | 0.02 | 0.05 | 0.10 | 0.20 |
| 0.04       | 7.1  | 7.1  | 7.2  | 7.0  | -1.22 | -1.13 | -1.19 | -1.13 | -0.17 | -0.15 | -0.15 | -0.15 | 1.79 | 1.89 | 1.81 | 1.86 | 1.49 | 1.24 | 1.24 | 1.53 |
| 0.06       | 7.1  | 7.1  | 7.2  | 7.5  | -0.77 | -0.88 | -1.01 | -1.09 | -0.21 | -0.20 | -0.20 | -0.20 | 1.77 | 1.85 | 1.94 | 1.98 | 0.72 | 0.75 | 0.92 | 1.19 |
| 0.08       | 7.1  | 7.0  | 7.0  | 7.5  | -0.50 | -0.65 | -0.83 | -1.01 | -0.24 | -0.24 | -0.22 | -0.22 | 1.69 | 1.74 | 1.90 | 1.95 | 0.49 | 0.64 | 0.82 | 1.02 |
| 0.10       | 7.0  | 6.9  | 6.8  | 7.4  | -0.37 | -0.49 | -0.69 | -0.92 | -0.25 | -0.25 | -0.23 | -0.22 | 1.61 | 1.65 | 1.87 | 1.88 | 0.52 | 0.70 | 0.85 | 0.96 |
| 0.20       | 6.7  | 6.4  | 6.3  | 6.8  | -0.66 | -0.59 | -0.64 | -0.83 | -0.11 | -0.15 | -0.18 | -0.17 | 1.47 | 1.44 | 1.81 | 1.58 | 1.10 | 1.17 | 1.29 | 1.28 |
| 0.30       | 7.4  | 7.2  | 7.0  | 7.4  | -1.19 | -1.03 | -0.95 | -1.04 | -0.01 | -0.08 | -0.14 | -0.16 | 1.40 | 1.31 | 1.67 | 1.56 | 1.51 | 1.58 | 1.69 | 1.79 |
| 0.40       | 8.8  | 8.4  | 8.2  | 8.4  | -1.63 | -1.45 | -1.34 | -1.34 | 0.03  | -0.05 | -0.13 | -0.17 | 1.29 | 1.20 | 1.55 | 1.63 | 2.00 | 2.12 | 2.19 | 2.36 |
| 0.60       | 12.3 | 11.2 | 11.0 | 10.8 | -2.29 | -2.13 | -2.06 | -1.95 | 0.02  | -0.08 | -0.16 | -0.23 | 1.28 | 1.23 | 1.48 | 1.75 | 3.11 | 3.34 | 3.31 | 3.40 |
| 0.80       | 15.8 | 14.0 | 13.9 | 13.4 | -2.78 | -2.60 | -2.58 | -2.40 | -0.02 | -0.14 | -0.22 | -0.29 | 1.51 | 1.55 | 1.66 | 1.85 | 4.13 | 4.33 | 4.17 | 4.07 |
| 1.00       | 19.0 | 16.6 | 16.5 | 15.7 | -3.17 | -2.90 | -2.87 | -2.65 | -0.08 | -0.22 | -0.30 | -0.36 | 1.81 | 1.97 | 2.01 | 2.02 | 4.94 | 4.99 | 4.67 | 4.39 |
| 2.00       | 31.0 | 27.8 | 23.8 | 22.5 | -4.44 | -3.50 | -2.68 | -2.52 | -0.27 | -0.49 | -0.55 | -0.56 | 2.70 | 3.30 | 4.33 | 3.92 | 6.73 | 6.18 | 5.29 | 4.53 |

corresponds to about 3 to 5 cycles later.

Figures 3, 4 and 5 present examples of  $T_{MAX}(T)$  computed from equation (1) for  $M=6.5$ ,  $\Delta=10,50$  and  $100$  km, respectively, for  $s=0$  and  $s=2$ ,  $p=0.5$  and for horizontal and vertical Pseudo Relative Velocity Spectra (PSV). It is seen that the maximum horizontal response for periods shorter than about 1 sec and for  $s=2$  all occur within one second from each other. The times of maxima for  $s=0$  and for vertical motions in general display gradual increase with increasing oscillator period; a possible consequence of relatively greater dispersion of waves leading to vertical components of ground motion and of wave propagating through alluvium and sedimentary layers.

In general, and for long period motions in particular, the times of maximum response increase with decreasing damping. The scatter of observed times also increases with decreasing damping (Figure 2). For  $\zeta=0.0$  this scatter is so large that it renders analysis in terms of equation (1) impractical.

#### Scaling in Terms of MMI, s, v and p

For scaling of  $T_{MAX}(T)$  in terms of Modified Mercalli Intensity at the recording station, we adopt

$$T_{MAX}(T),_p = a(T)p + b(T)s + c(T)I_{MM} + d(T)v \quad (2)$$

In this regression model, all scaling functions have the meaning analogous to that discussed in connection with equation (1).  $I_{MM}$  which here takes the place of  $M$  in equation (1) takes on numerical values 1, 2, 3, ..., and 12 and corresponds to discrete levels I, II, ..., and XII on the MMI scale.

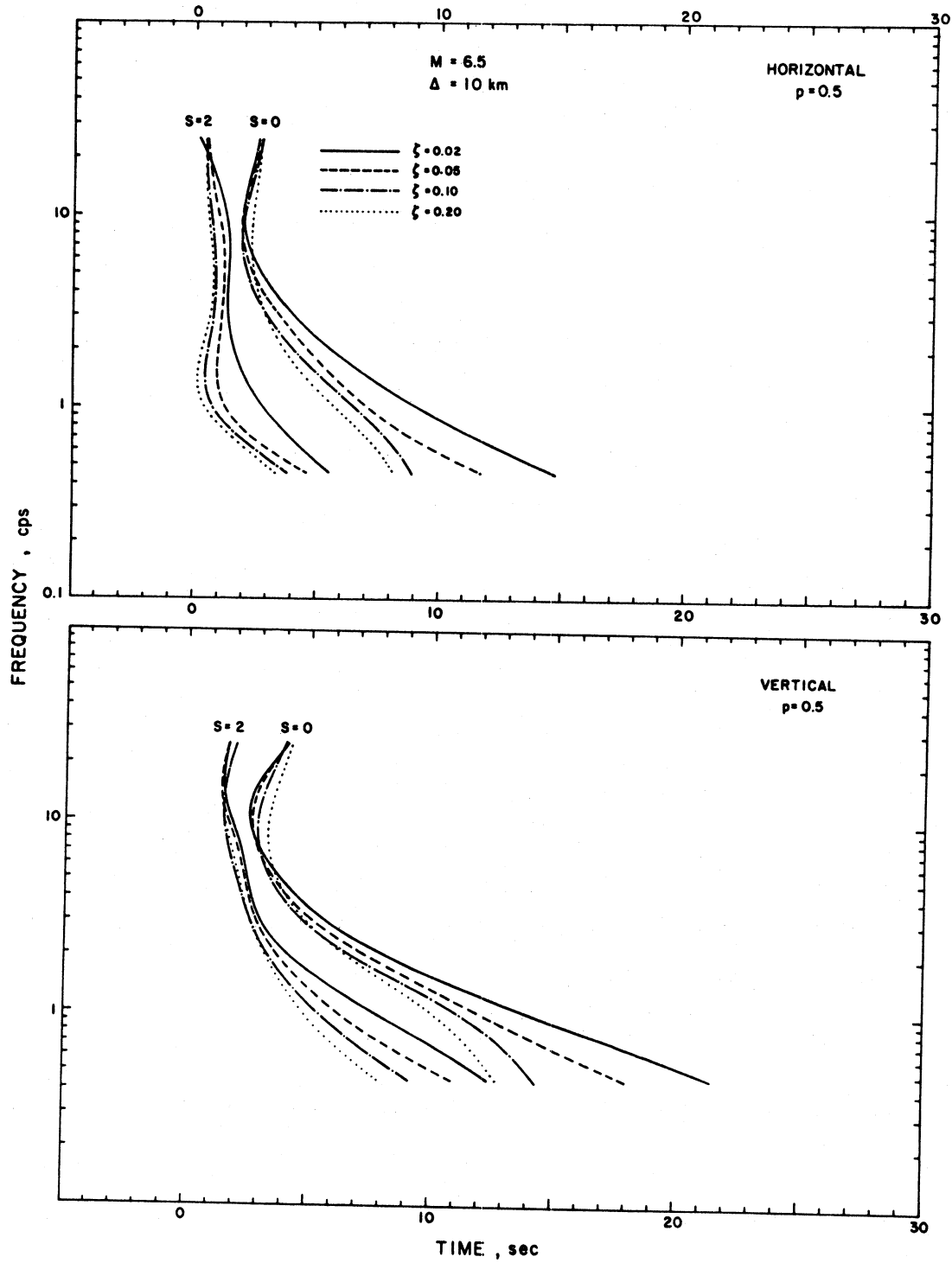


FIGURE 3

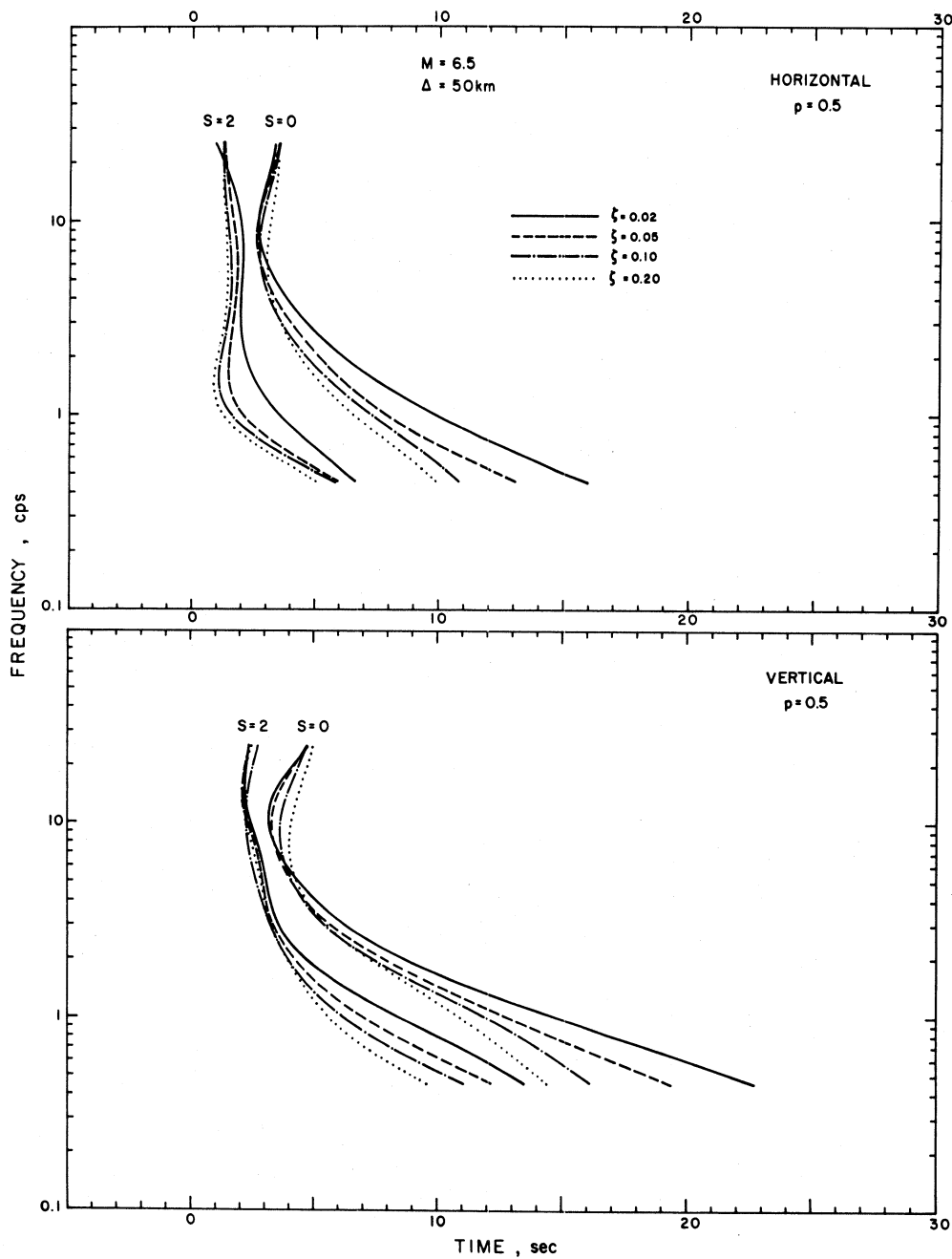


FIGURE 4

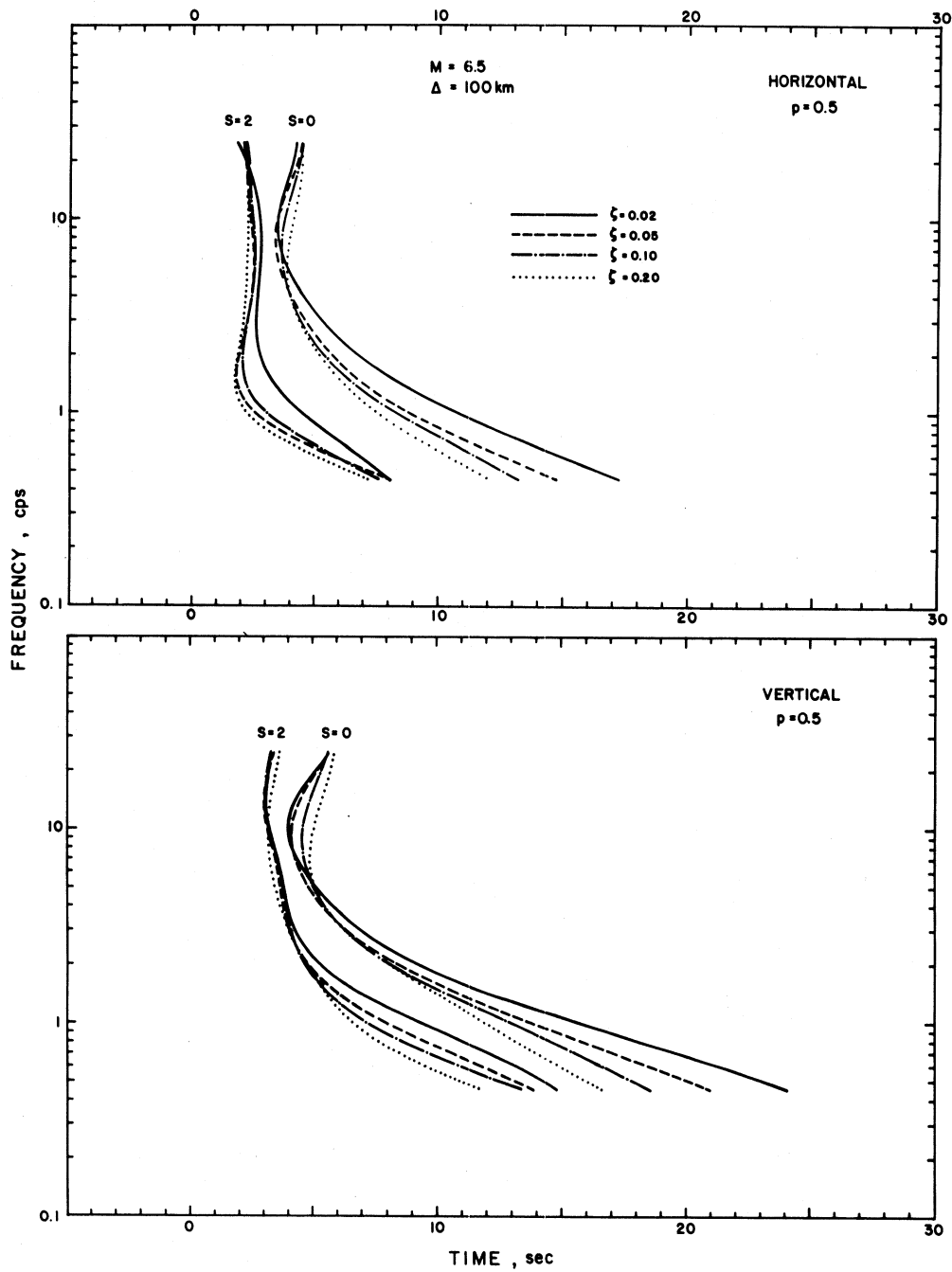


FIGURE 5

Figure 6 presents the smoothed coefficient functions  $a(T)$  through  $d(T)$  for  $\zeta = 0.02, 0.05, 0.10$  and  $0.20$ . Table II gives selected amplitudes of these functions at 11 periods.

Function  $a(T)$  has a similar shape as  $a(T)$  in Figure 2 but its amplitudes are larger by 3 to 10 seconds. This means that the regression represented by equation (2) leads to greater scatter of observed  $T_{MAX}(T)$  about the assumed model than in the correlations in terms of magnitude and epicentral distance. Functions  $b(T)$  and  $d(T)$  are essentially identical to their analogues  $b(T)$  and  $e(T)$  in Figure 2. Function  $c(T)$ , negative for all periods between 0.04 sec and 2 sec, results in a faster buildup of response for higher levels on MMI scale. This result is in good agreement with  $c(T)$  in Figure 2 and for correlations of  $T_{MAX}(T)$  with magnitude.

Figures 7, 8 and 9 present examples of  $T_{MAX}(T)$  plotted for MMI levels IV, VI and VIII, for  $p = 0.5$ , horizontal and vertical motions and for sites located on hard basement rock ( $s=2$ ) and alluvium ( $s=0$ ). Similar trends to those discussed for Figures 3, 4 and 5 are seen.

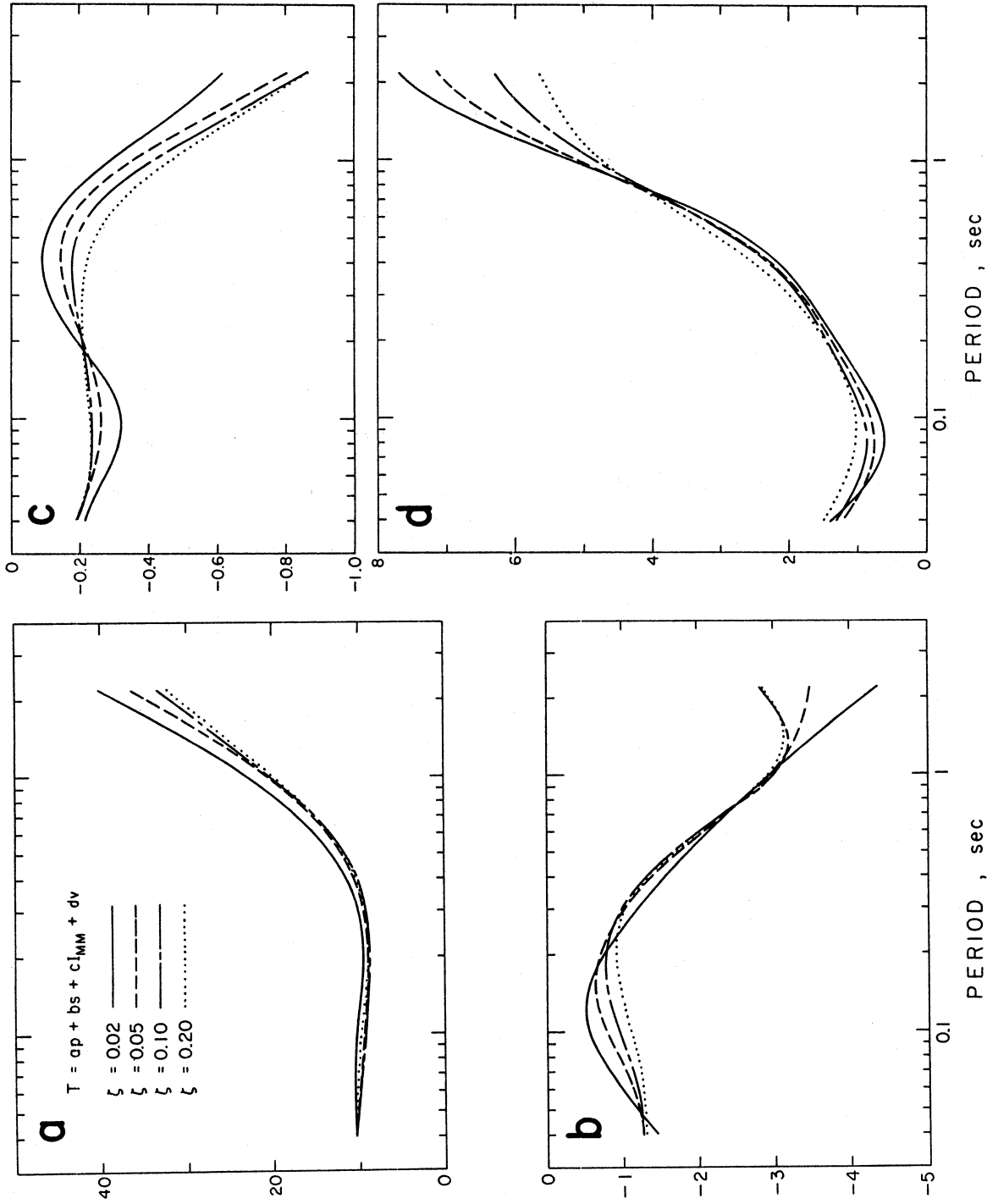


FIGURE 6

Functions  $a(T)$ ,  $b(T)$ ,  $\dots$  and  $d(T)$  in  
 $TMAX(T) = a(T)p + b(T)s + c(T)I_{MM} + d(T)v$

TABLE II

Regression Functions  $a(T)$  through  $d(T)$  in  $TMAX(T)$ ,  $p = a(T)p + b(T)s + c(T)I_{MM} + d(T)v$   
for Four Fractions of Critical Damping  $\zeta$

| T(sec) | a(T) |      |      | b(T) |      |      | c(T)  |       |       | d(T)  |       |       |       |      |      |      |      |
|--------|------|------|------|------|------|------|-------|-------|-------|-------|-------|-------|-------|------|------|------|------|
|        | 0.02 | 0.05 | 0.10 | 0.02 | 0.05 | 0.10 | 0.02  | 0.05  | 0.10  | 0.02  | 0.05  | 0.10  | 0.20  |      |      |      |      |
| 0.04   | 10.4 | 10.4 | 10.4 | 10.4 | 10.4 | 10.4 | -1.45 | -1.26 | -1.26 | -1.29 | -0.21 | -0.19 | -0.19 | 1.37 | 1.21 | 1.31 | 1.49 |
| 0.06   | 10.4 | 9.9  | 9.9  | 10.2 | 10.2 | 10.2 | -1.00 | -1.13 | -1.19 | -1.26 | -0.28 | -0.23 | -0.23 | 0.78 | 0.85 | 0.96 | 1.16 |
| 0.08   | 10.4 | 9.6  | 9.5  | 10.0 | 10.0 | 10.0 | -0.71 | -0.95 | -1.07 | -1.19 | -0.31 | -0.24 | -0.23 | 0.62 | 0.76 | 0.87 | 1.04 |
| 0.10   | 10.2 | 9.4  | 9.2  | 9.7  | 9.7  | 9.7  | -0.57 | -0.79 | -0.95 | -1.11 | -0.32 | -0.26 | -0.23 | 0.67 | 0.82 | 0.92 | 1.03 |
| 0.20   | 9.4  | 8.9  | 8.7  | 8.9  | 8.9  | 8.9  | -0.76 | -0.71 | -0.79 | -0.91 | -0.19 | -0.21 | -0.21 | 1.52 | 1.38 | 1.45 | 1.48 |
| 0.30   | 10.0 | 9.4  | 9.1  | 9.3  | 9.3  | 9.3  | -1.20 | -1.02 | -0.98 | -1.03 | -0.11 | -0.16 | -0.18 | 1.74 | 1.81 | 1.85 | 1.98 |
| 0.40   | 11.4 | 10.5 | 10.1 | 10.3 | 10.3 | 10.3 | -1.57 | -1.38 | -1.32 | -1.32 | -0.09 | -0.15 | -0.18 | 2.14 | 2.25 | 2.28 | 2.49 |
| 0.60   | 15.0 | 13.6 | 13.2 | 13.3 | 13.3 | 13.3 | -2.15 | -2.08 | -2.06 | -2.02 | -0.13 | -0.18 | -0.22 | 3.13 | 3.28 | 3.28 | 3.48 |
| 0.80   | 19.0 | 17.1 | 16.8 | 16.7 | 16.7 | 16.7 | -2.60 | -2.60 | -2.65 | -2.58 | -0.21 | -0.26 | -0.31 | 4.21 | 4.28 | 4.18 | 4.24 |
| 1.00   | 22.9 | 20.6 | 20.3 | 19.9 | 19.9 | 19.9 | -2.96 | -2.95 | -3.00 | -2.92 | -0.29 | -0.36 | -0.42 | 5.16 | 5.09 | 4.84 | 4.73 |
| 2.00   | 38.0 | 34.4 | 31.8 | 30.8 | 30.8 | 30.8 | -4.17 | -3.45 | -2.93 | -2.95 | -0.58 | -0.75 | -0.81 | 7.56 | 6.99 | 6.21 | 5.58 |

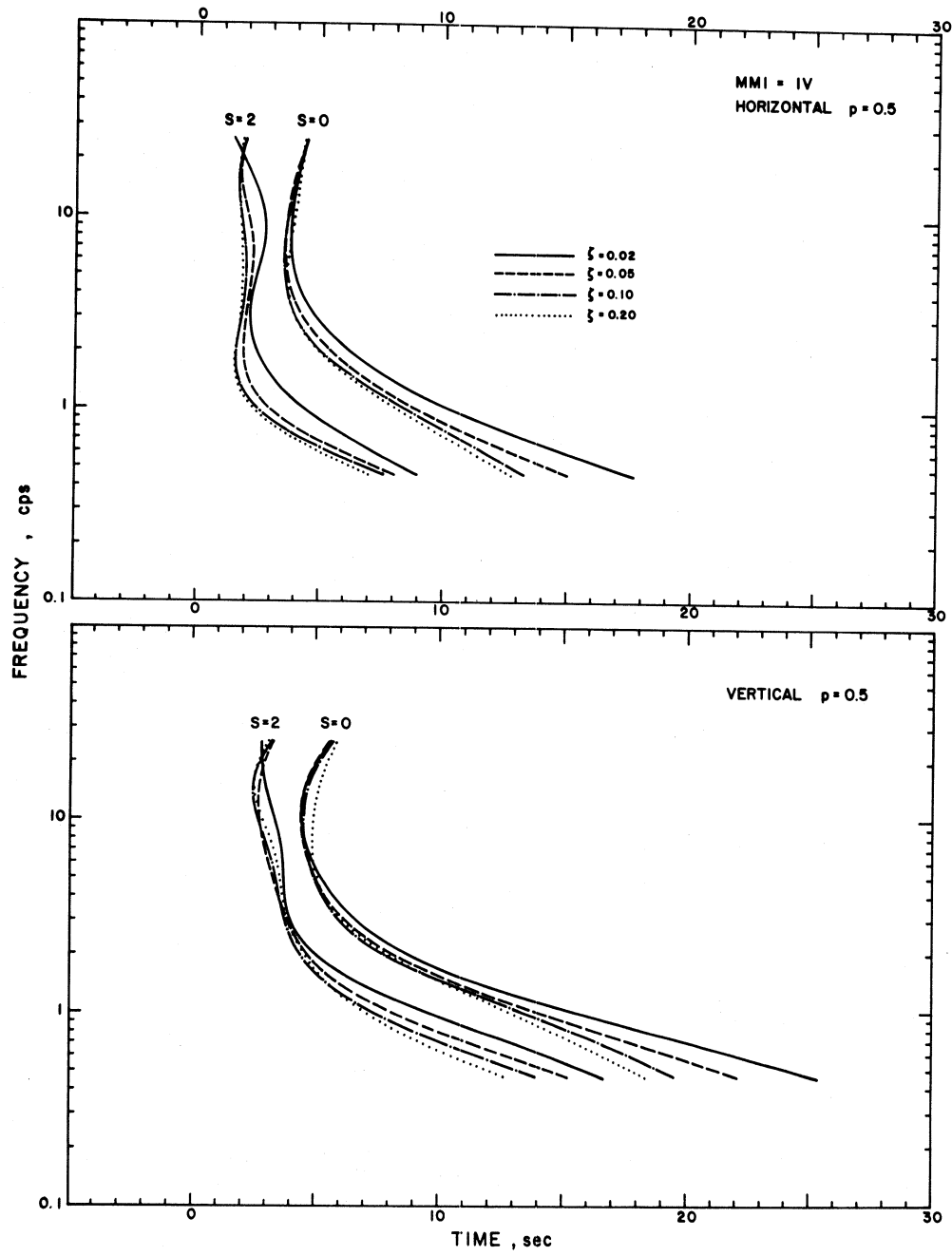


FIGURE 7

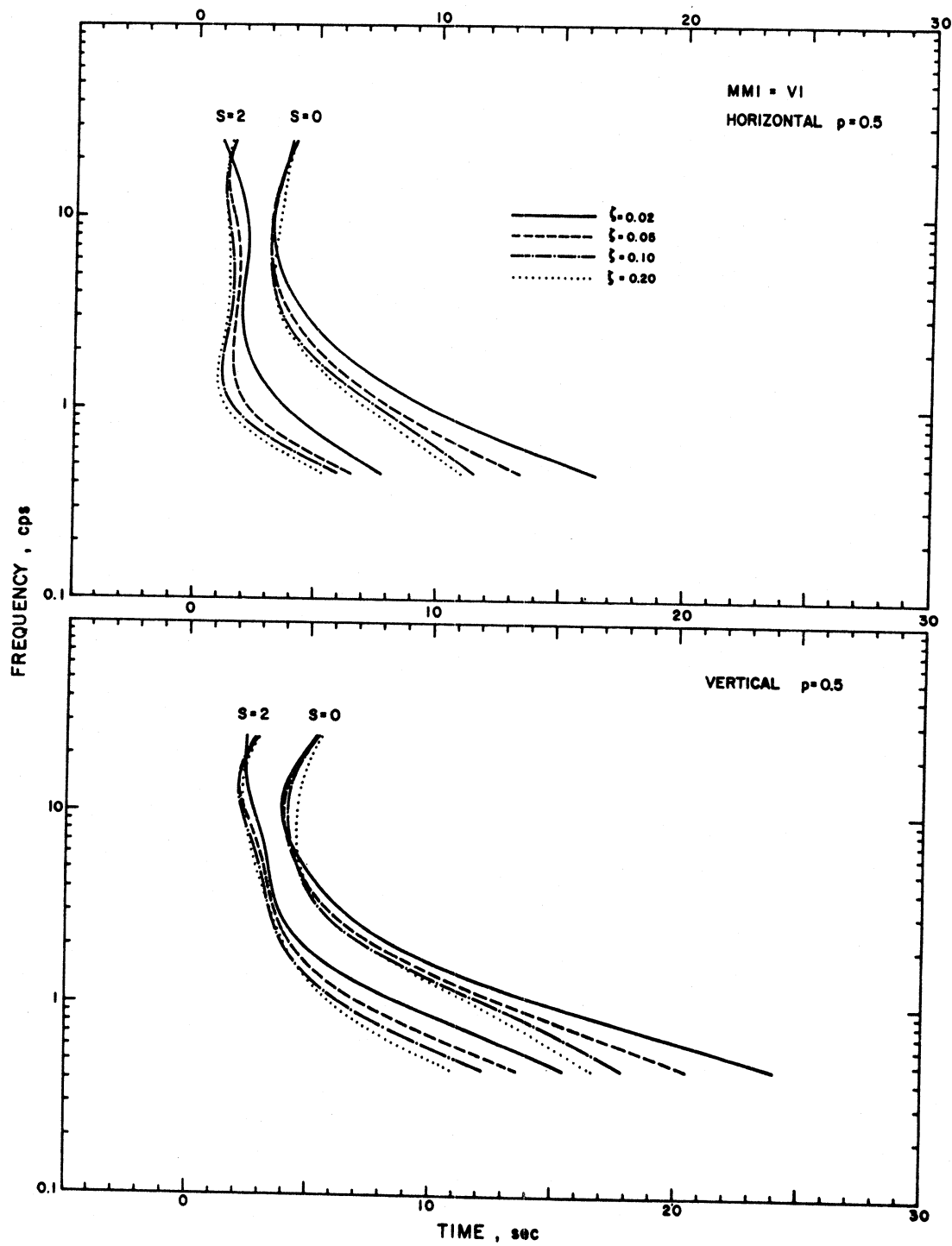


FIGURE 8

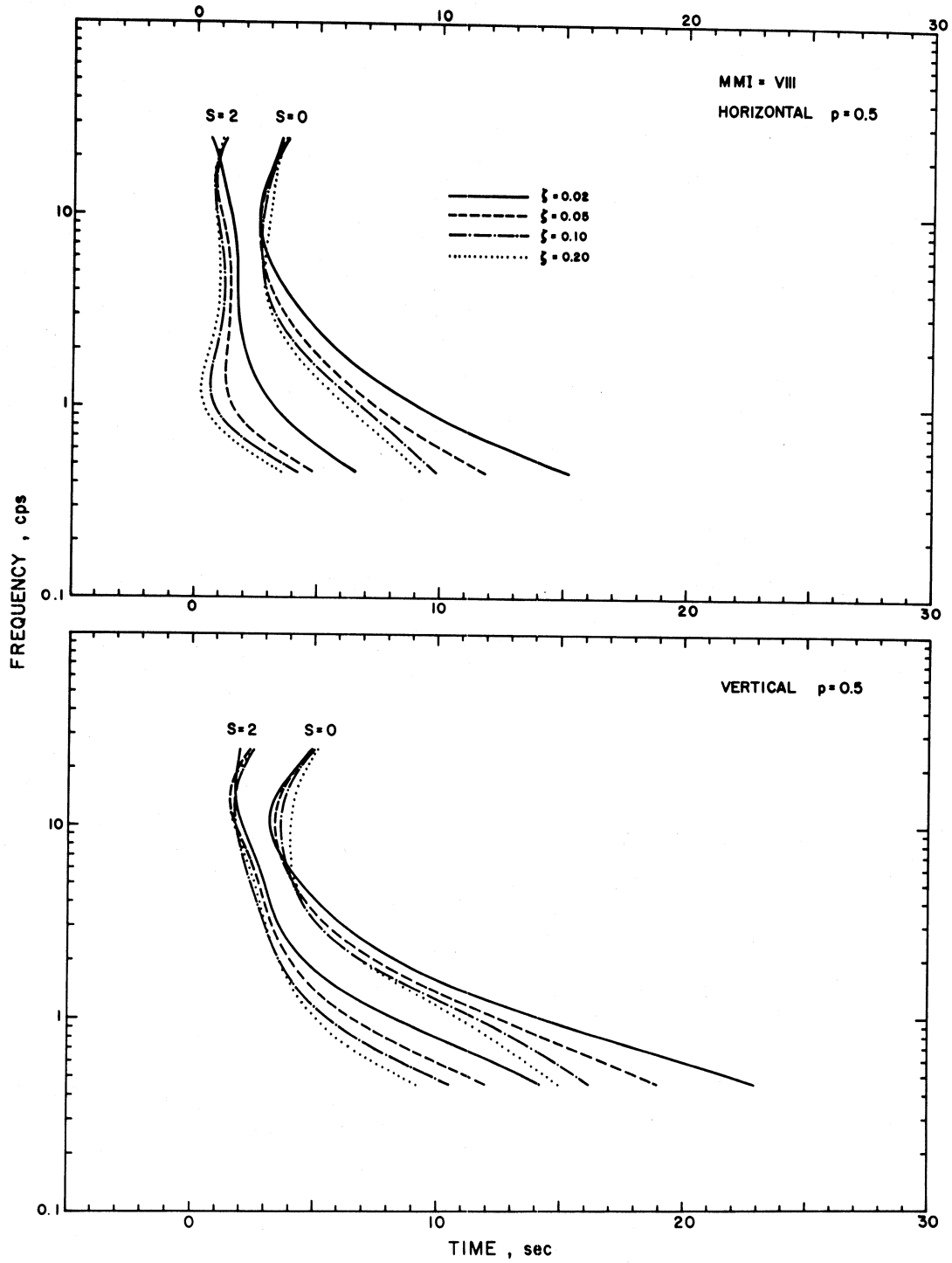


FIGURE 9

## DISTRIBUTION OF TIME OF MAXIMUM RESPONSE

The regression analyses of equations (1) and (2) have been performed by using a correlation function which is linear in an approximation to the probability of not exceeding  $T_{MAX}(T)$  when  $0.05 \leq p \leq 0.95$ . To emphasize this, from this point on, we refine the notation by adding a subscript " $\ell$ " so that  $p$  becomes  $p_\ell$ .

To describe the actual distribution, we calculate  $p_a$ , the actual fraction of data points for which the times of maxima are smaller than the predicted  $T_{MAX}(T)$ ,  $p_\ell$  for 9 values of the confidence level  $p_\ell = 0.1, 0.2, \dots, 0.9$  (Figures 10 and 11).  $p_a$  is then the empirically determined probability that  $T_{MAX}(T)$ ,  $p_\ell$  will not be exceeded.

As a convenience for future applications, we seek to have a simple analytical approximation relating  $p_a$  to  $p_\ell$  [9].

The statistical analyses of the time of maximum response of a linear oscillator suggest [1] an exponential or a sum of exponential distribution functions for  $p_a$  in terms of  $p_\ell$

$$p_a = F(p_\ell) = \int_{-\infty}^{p_\ell} f_1(x) dx$$

with the proposed probability function, for some  $x_0$ ,

$$f(x) = \begin{cases} -a_1 \beta_1 e^{\beta_1 x} + a_2 \beta_2 e^{\beta_2 x} & x > x_0 ; \beta_1, \beta_2 \leq 0 \\ 0 & x \leq x_0 \end{cases}$$

normalized to become a distribution function

$$f_1(x) = \begin{cases} f(x)/A & x > x_0 \\ 0 & x < x_0 \end{cases}$$

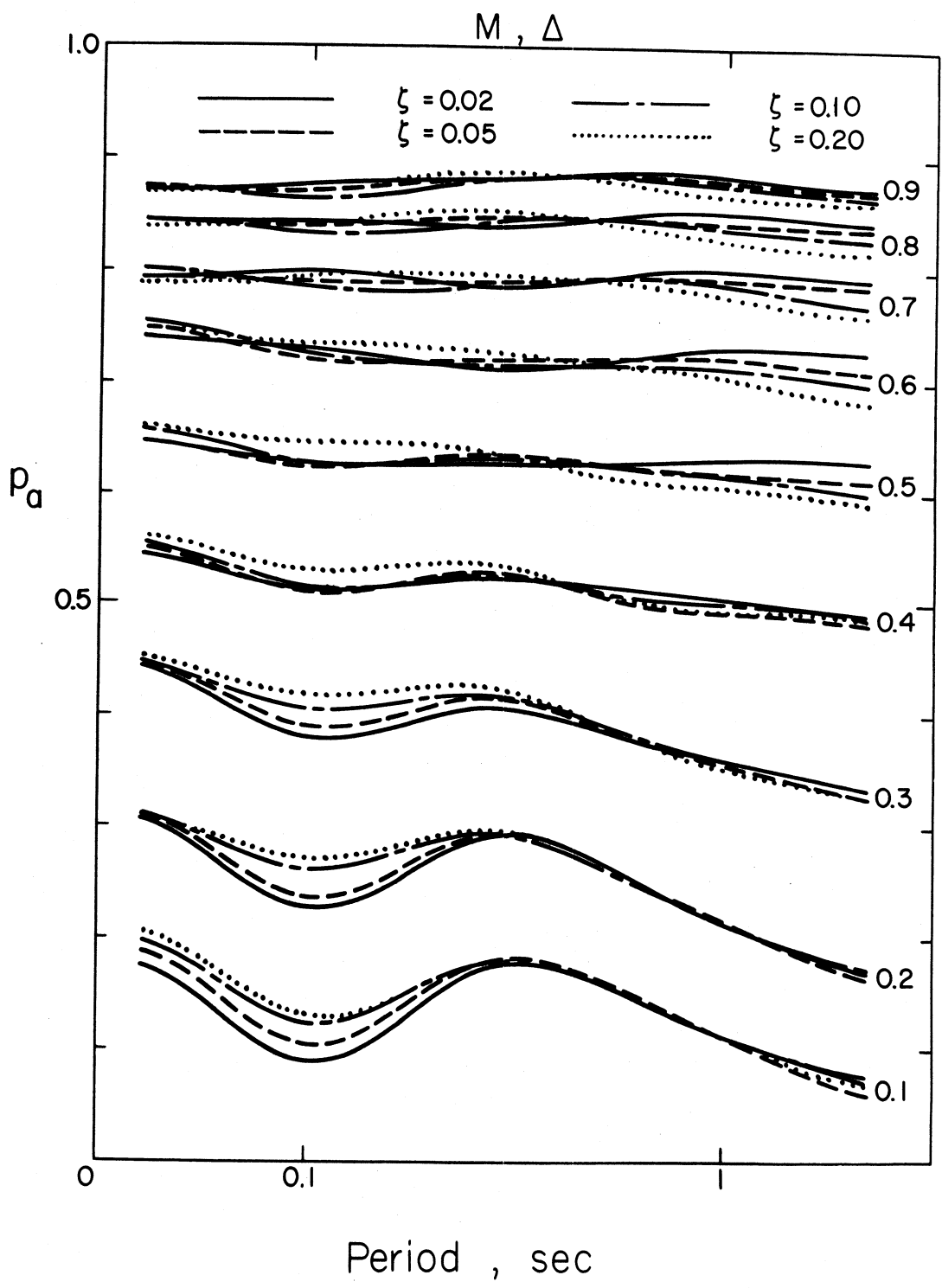


FIGURE 10

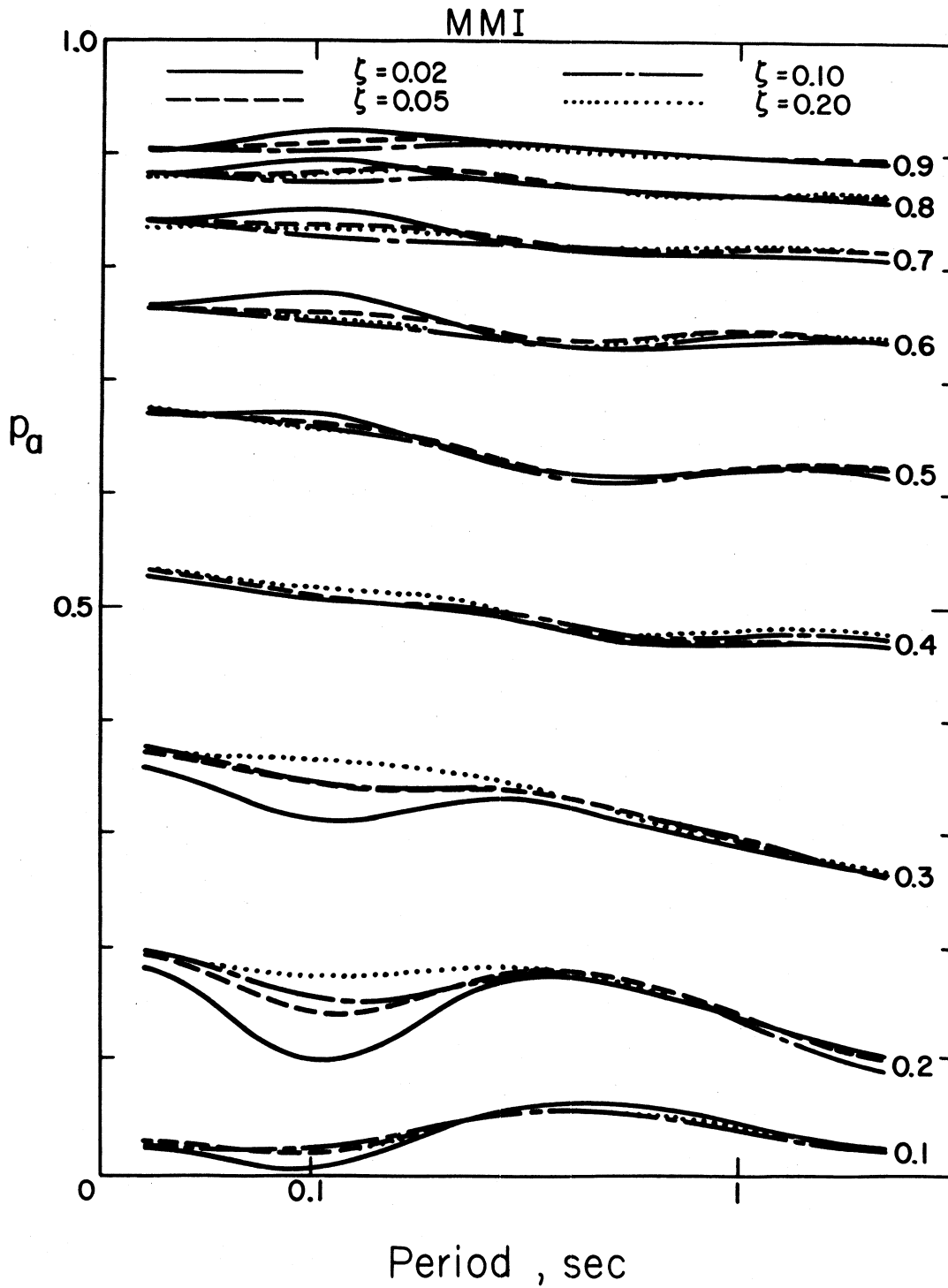


FIGURE 11

where

$$\begin{aligned} A &= \int_{-\infty}^{\infty} f(x) dx = \int_{x_0}^{\infty} f(x) dx = -a_1 e^{\beta_1 x} + a_2 e^{\beta_2 x} \Big|_{x_0}^{\infty} \\ &= a_1 e^{\beta_1 x_0} - a_2 e^{\beta_2 x_0} \end{aligned}$$

so that

$$\int_{-\infty}^{\infty} f_1(x) dx = \int_{x_0}^{\infty} f_1(x) dx = 1$$

Then for

$$\begin{aligned} p_a &= F(p_\ell) = \int_{-\infty}^{p_\ell} f_1(x) dx = \int_{x_0}^{p_\ell} f_1(x) dx \\ &= 1/A \int_{x_0}^{p_\ell} (-a_1 \beta_1 e^{\beta_1 x} + a_2 \beta_2 e^{\beta_2 x}) dx \quad (p_\ell > x_0) \\ &= 1/A (A - a_1 e^{\beta_1 p_\ell} + a_2 e^{\beta_2 p_\ell}) \end{aligned}$$

we get

$$p_a - F(p_\ell) = 1 - \alpha_1 e^{\beta_1 p_\ell} + \alpha_2 e^{\beta_2 p_\ell} \quad (3)$$

where

$$\alpha_1 = a_1/A$$

$$\alpha_2 = a_2/A$$

Equation (3) is then the scaling function of  $p_a$  versus  $p_\ell$ .

Figures 12 and 13 present the coefficients  $\alpha_1$ ,  $\alpha_2$ ,  $\beta_1$  and  $\beta_2$  in (3) which lead to acceptable fit of  $p_a$  versus  $p_\ell$ , for the data in Figures

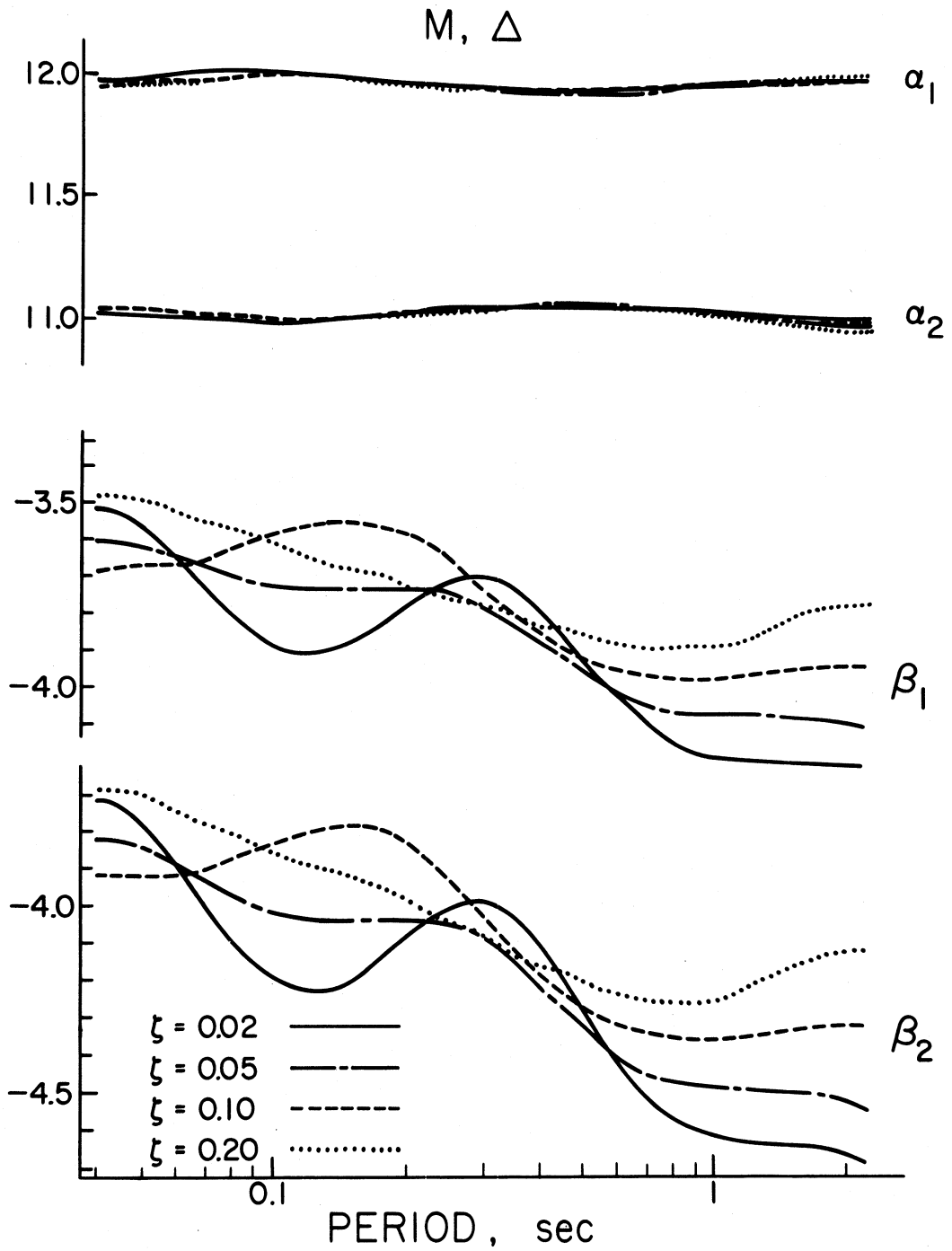


FIGURE 12

## MMI

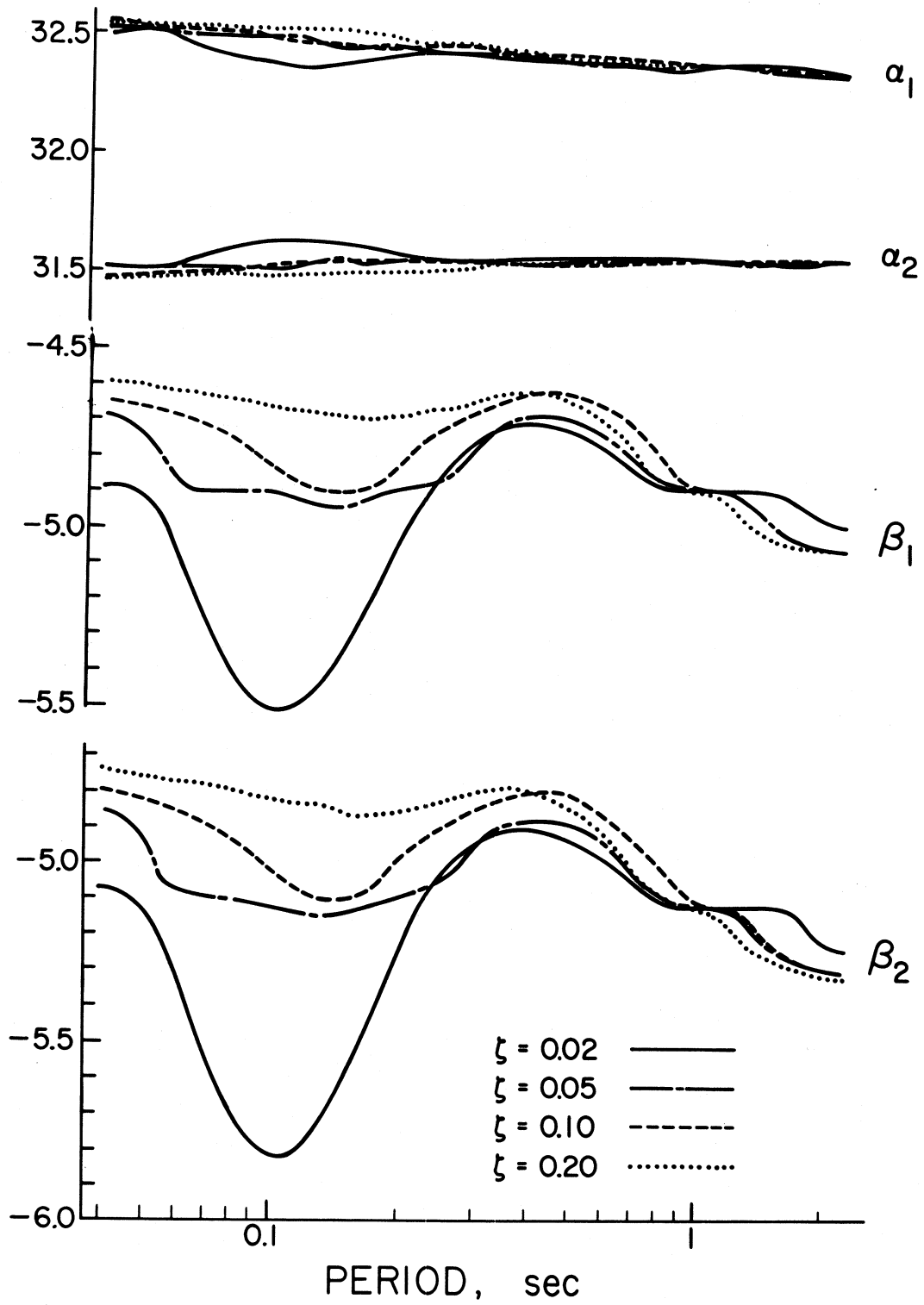


FIGURE 13

10 and 11. The corresponding  $\chi^2$  and Kolmogorov-Smirnov (K-S) tests and the computed values of  $\chi^2$  and maximum differences for K-S test (Figures 14 and 15) can be accepted with 95% confidence. Coefficients  $\alpha_1$ ,  $\alpha_2$ ,  $\beta_1$  and  $\beta_2$  are also presented in Tables III and IV to enable numerical evaluation of  $p_a$  versus  $p_\ell$  in (3).

This approximate characterization of  $p_a$  for models represented by equations (1) and (2) enables one to compute  $p_\ell$  (i.e.,  $p$  in equations (1) and (2)) from equation (3) for a chosen  $p_a$  and thus also to compute  $TMAX(T)_{p_\ell}$ . The functions  $\alpha_1$ ,  $\alpha_2$ ,  $\beta_1$  and  $\beta_2$  may prove to be useful for testing future theoretical models and calculations which will be aimed at better and more precise descriptions of the distribution of  $TMAX(T)$  than the present assumption involving superposition of exponential functions.

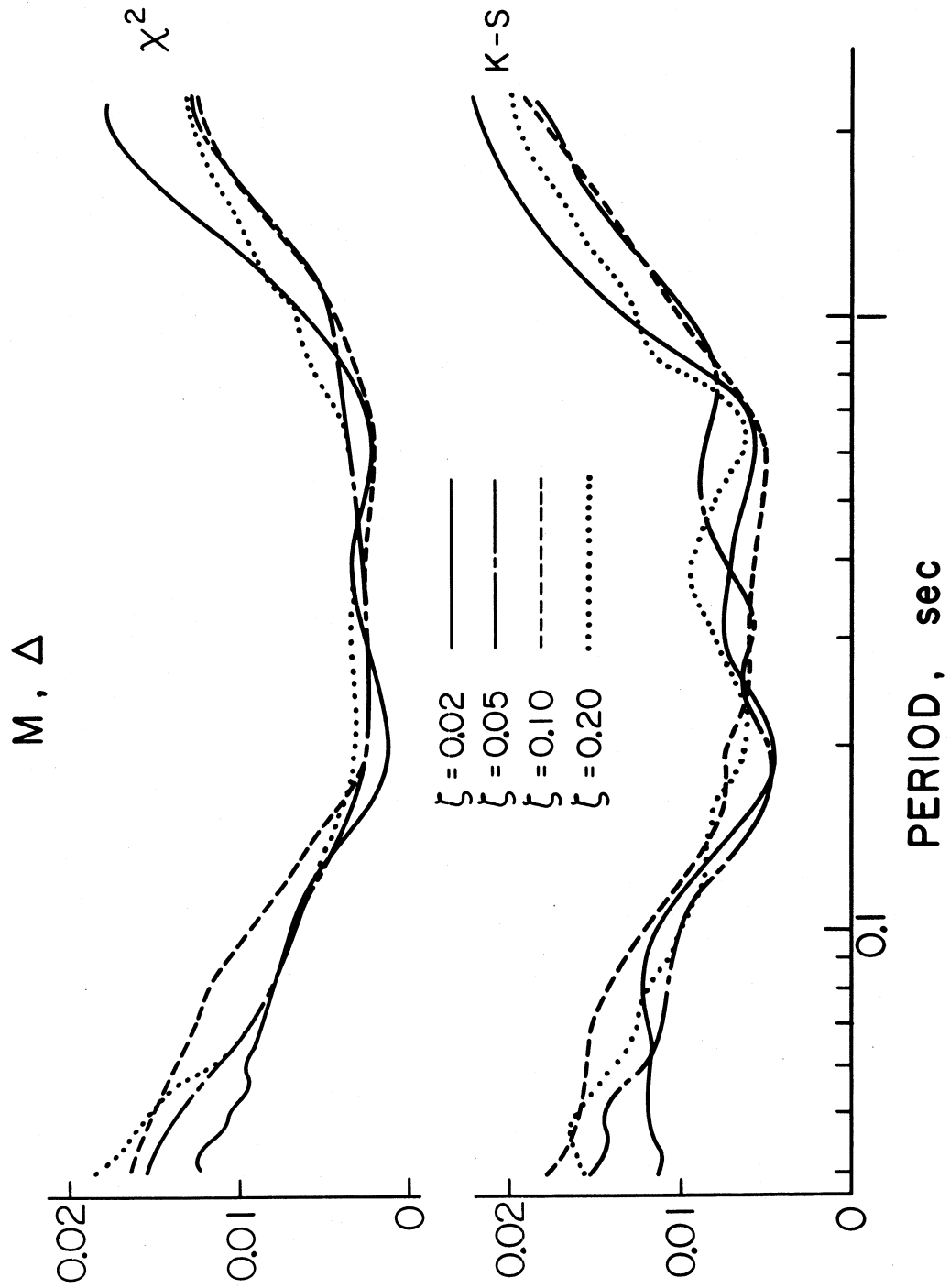


FIGURE 14

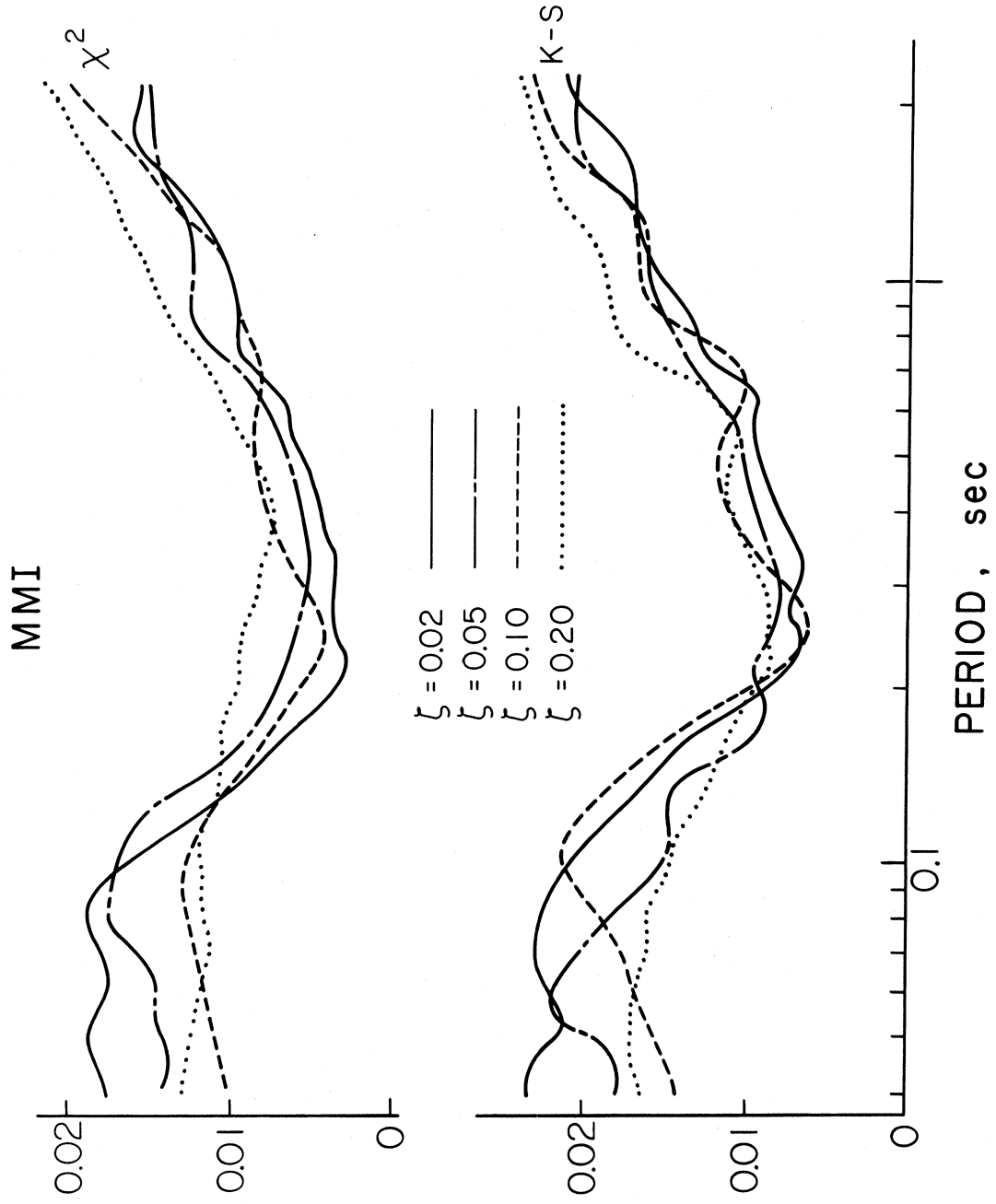


FIGURE 15

TABLE III

Coefficients  $\alpha_1$ ,  $\beta_1$ ,  $\alpha_2$  and  $\beta_2$  in  $p_a = 1 - \alpha_1 e^{\beta_1 p_\ell} + \alpha_2 e^{\beta_2 p_\ell}$ 

| $\zeta = 0.02$ |            |           |            |           | $\zeta = 0.05$ |            |           |            |           |
|----------------|------------|-----------|------------|-----------|----------------|------------|-----------|------------|-----------|
| T(sec)         | $\alpha_1$ | $\beta_1$ | $\alpha_2$ | $\beta_2$ | T(sec)         | $\alpha_1$ | $\beta_1$ | $\alpha_2$ | $\beta_2$ |
| 0.04           | 11.97      | -3.52     | 11.02      | -3.73     | 0.04           | 11.95      | -3.60     | 11.04      | -3.83     |
| 0.06           | 11.98      | -3.66     | 11.01      | -3.91     | 0.06           | 11.97      | -3.66     | 11.02      | -3.91     |
| 0.08           | 11.99      | -3.80     | 10.99      | -4.08     | 0.08           | 11.99      | -3.71     | 11.00      | -3.98     |
| 0.10           | 11.99      | -3.87     | 10.98      | -4.18     | 0.10           | 11.99      | -3.75     | 11.00      | -4.03     |
| 0.20           | 11.96      | -3.78     | 11.03      | -4.08     | 0.20           | 11.95      | -3.75     | 11.04      | -4.04     |
| 0.30           | 11.93      | -3.71     | 11.06      | -4.00     | 0.30           | 11.93      | -3.78     | 11.07      | -4.09     |
| 0.40           | 11.92      | -3.80     | 11.07      | -4.12     | 0.40           | 11.92      | -3.87     | 11.08      | -4.21     |
| 0.60           | 11.92      | -4.03     | 11.07      | -4.42     | 0.60           | 11.92      | -4.02     | 11.08      | -4.41     |
| 0.80           | 11.93      | -4.14     | 11.07      | -4.56     | 0.80           | 11.93      | -4.07     | 11.07      | -4.48     |
| 1.00           | 11.93      | -4.19     | 11.06      | -4.63     | 1.00           | 11.94      | -4.08     | 11.06      | -4.49     |
| 2.00           | 11.96      | -4.21     | 11.03      | -4.66     | 2.00           | 11.97      | -4.10     | 11.02      | -4.53     |

| $\zeta = 0.10$ |            |           |            |           | $\zeta = 0.20$ |            |           |            |           |
|----------------|------------|-----------|------------|-----------|----------------|------------|-----------|------------|-----------|
| T(sec)         | $\alpha_1$ | $\beta_1$ | $\alpha_2$ | $\beta_2$ | T(sec)         | $\alpha_1$ | $\beta_1$ | $\alpha_2$ | $\beta_2$ |
| 0.04           | 11.94      | -3.69     | 11.04      | -3.93     | 0.04           | 11.95      | -3.49     | 11.04      | -3.70     |
| 0.06           | 11.96      | -3.68     | 11.03      | -3.93     | 0.06           | 11.96      | -3.56     | 11.02      | -3.78     |
| 0.08           | 11.98      | -3.62     | 11.00      | -3.86     | 0.08           | 11.98      | -3.56     | 11.00      | -3.78     |
| 0.10           | 1.99       | -3.61     | 11.00      | -3.85     | 0.10           | 11.99      | -3.62     | 10.99      | -3.85     |
| 0.20           | 11.96      | -3.60     | 11.03      | -3.85     | 0.20           | 11.96      | -3.73     | 11.03      | -3.99     |
| 0.30           | 11.93      | -3.74     | 11.06      | -4.03     | 0.30           | 11.93      | -3.80     | 11.06      | -4.10     |
| 0.40           | 11.93      | -3.84     | 11.07      | -4.17     | 0.40           | 11.93      | -3.84     | 11.07      | -4.16     |
| 0.60           | 11.93      | -3.95     | 11.07      | -4.32     | 0.60           | 11.93      | -3.89     | 11.06      | -4.25     |
| 0.80           | 11.94      | -3.98     | 11.06      | -4.36     | 0.80           | 11.94      | -3.89     | 11.05      | -4.26     |
| 1.00           | 11.96      | -3.98     | 11.04      | -4.36     | 1.00           | 11.96      | -3.89     | 11.04      | -4.26     |
| 2.00           | 11.98      | -3.94     | 11.01      | -4.32     | 2.00           | 11.98      | -3.78     | 10.99      | -4.13     |

TABLE IV

Coefficients  $\alpha_1$ ,  $\beta_1$ ,  $\alpha_2$  and  $\beta_2$  in  $p_a = 1 - \alpha_1 e^{\beta_1 p_\ell} + \alpha_1 e^{\beta_2 p_\ell}$   
(MMI Model)

| $\zeta = 0.02$ |            |           |            |           | $\zeta = 0.05$ |            |           |            |           |
|----------------|------------|-----------|------------|-----------|----------------|------------|-----------|------------|-----------|
| T(sec)         | $\alpha_1$ | $\beta_1$ | $\alpha_2$ | $\beta_2$ | T(sec)         | $\alpha_1$ | $\beta_1$ | $\alpha_2$ | $\beta_2$ |
| 0.04           | 32.49      | -4.90     | 31.51      | -5.10     | 0.04           | 32.52      | -4.70     | 31.48      | -4.86     |
| 0.06           | 32.46      | -5.10     | 31.54      | -5.33     | 0.06           | 32.48      | -4.90     | 31.52      | -5.10     |
| 0.08           | 32.41      | -5.40     | 31.60      | -5.69     | 0.08           | 32.49      | -4.90     | 31.51      | -5.10     |
| 0.10           | 32.38      | -5.51     | 31.63      | -5.83     | 0.10           | 32.48      | -4.90     | 31.52      | -5.11     |
| 0.20           | 32.42      | -5.03     | 31.59      | -5.27     | 0.20           | 32.44      | -4.89     | 31.56      | -5.11     |
| 0.30           | 32.43      | -4.75     | 31.57      | -4.96     | 0.30           | 32.43      | -4.75     | 31.57      | -4.95     |
| 0.40           | 32.42      | -4.71     | 31.58      | -4.92     | 0.40           | 32.43      | -4.69     | 31.57      | -4.89     |
| 0.60           | 32.40      | -4.76     | 31.60      | -4.99     | 0.60           | 32.41      | -4.73     | 31.59      | -4.95     |
| 0.80           | 32.39      | -4.88     | 31.61      | -5.12     | 0.80           | 32.39      | -4.88     | 31.61      | -5.12     |
| 1.00           | 32.39      | -4.88     | 31.61      | -5.12     | 1.00           | 32.40      | -4.88     | 31.60      | -5.12     |
| 2.00           | 32.39      | -4.97     | 31.61      | -5.24     | 2.00           | 32.38      | -5.03     | 31.62      | -5.31     |

| $\zeta = 0.10$ |            |           |            |           | $\zeta = 0.20$ |            |           |            |           |
|----------------|------------|-----------|------------|-----------|----------------|------------|-----------|------------|-----------|
| T(sec)         | $\alpha_1$ | $\beta_1$ | $\alpha_2$ | $\beta_2$ | T(sec)         | $\alpha_1$ | $\beta_1$ | $\alpha_2$ | $\beta_2$ |
| 0.04           | 32.53      | -4.65     | 31.47      | -4.81     | 0.04           | 32.53      | -4.60     | 31.47      | -4.75     |
| 0.06           | 32.51      | -4.69     | 31.48      | -4.86     | 0.06           | 32.52      | -4.62     | 31.47      | -4.78     |
| 0.08           | 32.50      | -4.74     | 31.50      | -4.92     | 0.08           | 32.52      | -4.64     | 31.48      | -4.81     |
| 0.10           | 32.47      | -4.89     | 31.53      | -5.10     | 0.10           | 32.52      | -4.66     | 31.48      | -4.83     |
| 0.20           | 32.45      | -4.77     | 31.54      | -4.97     | 0.20           | 32.48      | -4.68     | 31.52      | -4.86     |
| 0.30           | 32.45      | -4.67     | 31.55      | -4.86     | 0.30           | 32.46      | -4.63     | 31.54      | -4.81     |
| 0.40           | 32.44      | -4.62     | 31.56      | -4.81     | 0.40           | 32.44      | -4.61     | 31.56      | -4.81     |
| 0.60           | 32.43      | -4.66     | 31.57      | -4.87     | 0.60           | 32.42      | -4.70     | 31.58      | -4.91     |
| 0.80           | 32.42      | -4.77     | 31.58      | -4.99     | 0.80           | 32.40      | -4.88     | 31.60      | -5.12     |
| 1.00           | 32.41      | -4.88     | 31.59      | -5.12     | 1.00           | 32.41      | -4.88     | 31.60      | -5.12     |
| 2.00           | 32.38      | -5.03     | 31.62      | -5.30     | 2.00           | 32.38      | -5.04     | 31.62      | -5.32     |

## CONCLUSIONS

In this paper we have attempted to describe the time at which the single-degree-of-freedom viscously damped oscillator reaches its maximum response during excitation corresponding to recorded earthquake shaking. Two simple regression models have been presented for scaling in terms of earthquake magnitude or Modified Mercalli Intensity at the recording station. The effects of epicentral distance, geologic conditions surrounding the station, horizontal or vertical direction of response and the distribution of times when the maxima occur have also been considered. The principal findings of this work can be summarized as follows:

- 1) Horizontal response amplitudes reach their maxima within several seconds after the S-wave arrival for periods shorter than about 4 seconds for stations located on hard rock and for epicentral distance less than 20 to 30 km. For every additional 50 km in epicentral distance, maximum response is delayed by approximately one additional second.
- 2) The times of maximum vertical response typically occur later by 1 (for periods near 0.1 sec) to 5 (for periods near 1 to 2 sec) seconds after horizontal response had reached its maximum.

#### ACKNOWLEDGEMENTS

We thank J.G. Anderson and H.L. Wong for critical reading of the manuscript and for useful suggestions and comments.

This work was supported by a contract from the U.S. Nuclear Regulatory Commission.

## REFERENCES

1. Crandal, S.H. (1970). First-Crossing Probabilities of the Linear Oscillator, *J. Sound Vib.* 12, (3) 285-299.
2. Trifunac, M.D. (1971). Response Envelope Spectrum and Interpretation of Strong Earthquake Ground Motion, *Bull. Seism. Soc. Amer.*, 61, 343-356.
3. Trifunac, M.D., and V.W. Lee (1973). Routine Computer Processing of Strong Motion Accelerograms, *Earthquake Eng. Res. Lab. EERL 73-03*, Calif. Inst. of Tech., Pasadena.
4. Trifunac, M.D., and A.G. Brady (1975). On the Correlation of Seismic Intensity Scales with the Peaks of Recorded Strong Ground Motion, *Bull. Seism. Soc. Amer.*, 65, 139-162.
5. Trifunac, M.D. (1976). Preliminary Empirical Model for Scaling Fourier Amplitude Spectra of Strong Ground Acceleration in Terms of Earthquake Magnitude, Source to Station Distance and Recording Site Conditions, *Bull. Seism. Soc. Amer.*, 66, 1343-1373.
6. Trifunac, M.D., and B.D. Westermo (1976a). Dependence of Duration of Strong Earthquake Ground Motion on Magnitude, Epicentral Distance, Geologic Conditions at the Recording Station and Frequency of Motion, *Dept. of Civil Eng., Report No. 76-02*, U.S.C., Los Angeles.
7. Trifunac, M.D., and B.D. Westermo (1976b). Correlations of Frequency Dependent Duration of Strong Earthquake Ground Motion with Modified Mercalli Intensity and the Geologic Conditions at the Recording Stations, *Dept. of Civil Eng., Report No. 76-03*, U.S.C., Los Angeles.
8. Trifunac, M.D. (1978). Preliminary Empirical Model for Scaling Fourier Amplitude Spectra of Strong Motion Acceleration in Terms of Modified Mercalli Intensity and Geologic Site Conditions, *Int. J. Earthquake Eng. and Struct. Dyn.*, (in press).
9. Trifunac, M.D. (1978). Response Spectra of Earthquake Ground Motion, *J. Eng. Mech. Div., ASCE, EM5, Vol. 104*, 1081-1097.